

Sparse Quantum State Preparation for Strongly Correlated Systems

César Feniou,^{†,‡} Olivier Adjoua,[†] Baptiste Claudon,^{†,‡} Julien Zylberman,[¶]
Emmanuel Giner,[†] and Jean-Philip Piquemal^{*,†,‡}

[†]*Sorbonne Université, LCT, UMR 7616 CNRS, Paris, France*

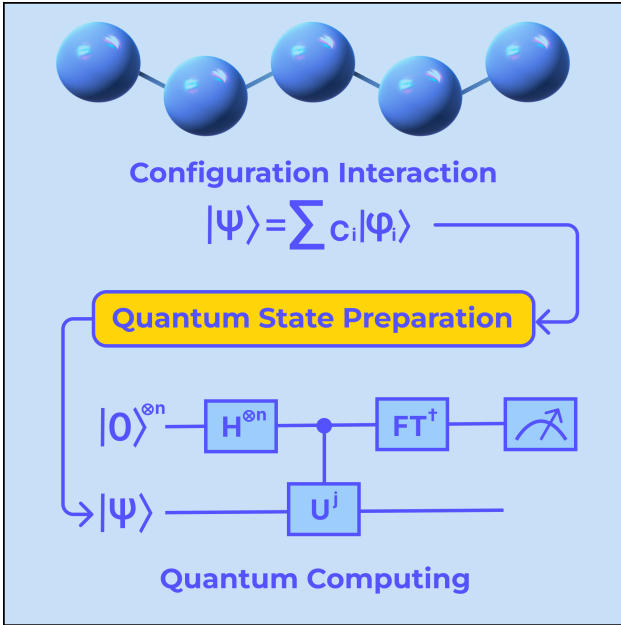
[‡]*Qubit Pharmaceuticals, Advanced Research Department, Paris, France*

[¶]*Sorbonne Université, LERMA, UMR 8112 CNRS, Paris, France*

E-mail: jean-philip.piquemal@sorbonne-universite.fr

Abstract

Quantum Computing allows, in principle, the encoding of the exponentially scaling many-electron wave function onto a linearly scaling qubit register, offering a promising solution to overcome the limitations of traditional quantum chemistry methods. An essential requirement for ground state quantum algorithms to be practical is the initialisation of the qubits to a high-quality approximation of the sought-after ground state. Quantum State Preparation (QSP) allows the preparation of approximate eigenstates obtained from classical calculations, but it is frequently treated as an oracle in quantum information. In this study, we conduct QSP on the ground state of prototypical strongly correlated systems, up to 28 qubits, using the Hyperion GPU-accelerated state-vector emulator. Various variational and non-variational methods are compared in terms of their circuit depth and classical complexity. Our results indicate that the recently developed Overlap-ADAPT-VQE algorithm offers the most advantageous performance for near-term applications.



Simulating electronic structure on computers is a crucial and challenging endeavor with significant applications in drug discovery and advanced materials design.¹ Unfortunately, the full configuration interaction (FCI) method, which is capable of providing exact solutions to the electronic time-independent non-relativistic Schrödinger equation in a given basis, requires the diagonalisation of the molecular Hamiltonian to solve the electronic structure problem. The computational cost of performing an FCI calculation therefore increases exponentially as the system size expands. Quantum computers offer a promising solution to overcome this issue by enabling the representation and manipulation of exponentially large electronic wave functions using only a linear number of qubits. To leverage the potential of quantum computers for such tasks, quantum algorithms such as the Variational Quantum Eigensolver² (VQE) and Quantum Phase Estimation^{3,4} (QPE) have been developed for ground state quantum chemistry calculations.⁵⁻⁷

Unfortunately, the limited quantum resources available on current-generation Noisy Intermediate Scale Quantum (NISQ) devices severely limit the implementation of such methods and their ability to achieve an advantage over their classical counterparts. Hence, there is a need for the simultaneous use of both improved quantum hardware and resource-efficient

quantum algorithms. Both VQE and QPE have a significantly reduced computational cost when the initial state, i.e. the starting configuration of qubits, is carefully prepared in order to exhibit high overlap with the ground state of the system under study. Since VQE is an optimization problem, beginning with an initial state that is near the solution naturally enhances the efficiency of the search for the optimal solution. Regarding QPE, the success probability of the algorithm is proportional to the overlap between the initial state and the Hamiltonian ground state being simulated.^{3,4} For a typical chemical quantum simulation, the Hartree-Fock state is usually chosen as initial state for two main reasons: it can be represented on a quantum computer using just a few quantum gates, and it tends to be the predominant Slater determinant for most molecular systems. However, as pointed out in many studies,⁷⁻¹⁰ a single-determinant initial state might not be accurate enough for quantum computation of strongly correlated systems. One possible strategy to generate more accurate and multireference initial states is to build upon the ability of conventional quantum chemistry methods to produce such wave functions. The subsequent step involves transferring this classical data into the quantum computer to prepare the desired initial state, a process known as Quantum State Preparation (QSP).¹¹ QSP is the prevalent 'black-box' or oracle procedure in quantum information. Formally, it involves preparing the state $|\Psi\rangle$ from a set of coefficients c_p such as :

$$|\Psi\rangle = \sum_{p \in \{0,1\}^n} c_p |p\rangle, \quad \sum_{p \in \{0,1\}^n} |c_p|^2 = 1. \quad (1)$$

Note that the QSP of an arbitrary target state necessitates circuits that scale exponentially with the number of qubits either in size, depth or number of ancilla qubits.¹¹⁻¹³ Consequently, QSP could potentially dominate the overall computational cost of the quantum algorithm, leading to the loss of the anticipated advantage. An usual metric for assessing quantum resource requirements is the CNOT (Controlled-NOT) gates count. CNOTs involve two-qubit operations and are typically costlier in terms of physical qubits and worse in fidelity

than one-qubit operations.

Configuration interaction¹⁴ (CI) is a post-Hartree-Fock quantum chemistry approach that represents the wave function as a weighted linear combination of Slater determinants. As the size of the FCI space grows exponentially with the number of particles and basis functions, the Selected-CI (SCI) methods have been proposed in order to select automatically only the important contributions in the Hilbert space. Among various flavors of SCI, the CI perturbatively selected iteratively (CIPSI)^{15,16} employs an iterative approach in which the most pertinent Slater determinant are dynamically added to the wave function based on an importance obtained derived from perturbation theory (PT). By choosing on-the-fly Slater determinants tailored to the systems being simulated, the SCI ansatz wave function rapidly captures the bulk of correlation effects and is therefore a natural candidate for a suitable multi-reference initial quantum states. Formally, the SCI wave function is defined over a subset of Slater determinants within the FCI space, denoted here the variational subset of determinants $\mathcal{V} = \{|\phi_i\rangle, i = 1, N\}$, and the energy is minimized over this set of parameters

$$\begin{aligned} |\Psi_{\text{SCI}}\rangle &= \sum_{i \in \mathcal{V}} c_i |\phi_i\rangle, \\ \{c_i\} &= \text{argmin} \frac{\langle \Psi_{\text{SCI}} | H | \Psi_{\text{SCI}} \rangle}{\langle \Psi_{\text{SCI}} | \Psi_{\text{SCI}} \rangle}. \end{aligned} \quad (2)$$

For a given wave function $|\Psi_{\text{SCI}}\rangle$, one can compute the associated second-order perturbed energy as

$$E^{(2)} = \sum_{I \notin \mathcal{V}} \frac{\langle I | H | \Psi_{\text{SCI}} \rangle^2}{E(\Psi_{\text{SCI}}) - E(I)}, \quad (3)$$

where $E(\Psi)$ is the variational energy of a given wave function Ψ . Therefore, the quantity $E^{(2)}$ is a measure of the remaining contribution to the energy of the Slater determinants not already captured in $|\Psi_{\text{SCI}}\rangle$. In the following calculations, we stop our calculations when $|E^{(2)}| < 10^{-4}$ in order to obtain target states of near FCI quality.

The process of encoding CI states in qubit registers involves mapping Slater determinants to computational basis states. The Jordan-Wigner fermion-to-qubit transformation¹⁷

is commonly employed for this mapping. In this transformation, each qubit stores the occupation of a spin-orbital, meaning that each vector in the computational basis corresponds to a Slater determinant. Computational basis states can represent unphysical states, like the $|0\rangle^n$ state, which corresponds to a configuration with zero particles. The Hartree-fock state of an m -electron and n -spin-orbital system is encoded as $|\Psi_{\text{HF}}\rangle = |1\rangle^m \otimes |0\rangle^{n-m}$, when arranging the spin-orbitals in increasing order of energy. Firstly, let us remark that the SCI target state has a number of variational determinants M much smaller than the dimension of the computational Hilbert space ($M \ll 2^n$). It is thus encoded as a *sparse quantum state* of sparsity M . Second, more generally, let us remark that it respects multiple fundamental symmetries such as fermionic anticommutation relations, which are reflected in the amplitudes, particle conservation and projected-spin, with only specific computational basis states respecting them. The molecular hamiltonian eigenstates thus belong to a subspace of the n -qubit Hilbert space that is relevant to these symmetries.

Having established the properties of the target wave functions, we can now shift our attention to exploring the diverse methods available for quantum state preparation of such targets. One first natural idea was introduced by Gard et. al.¹⁸ and involves fully parameterising the symmetry-preserving subspace with minimal CNOT count. Parameters are then variationally tuned until convergence to the target state which is within this subspace. Assuming convergence, this Symmetry-Preserving-VQE approach allows for an exact state preparation with a maximum CNOT count of three times the dimension of the subspace. An established alternative to fixed circuit methods involves adaptive variational algorithms where quantum circuits are grown tailored to the problem being simulated. The Adaptive Derivative-Assembled Pseudo Trotter (ADAPT)-VQE¹⁹ belongs to this family of methods, and has become a benchmark technique due to its capability of generating ansatz wave functions that are both highly accurate approximations to the ground state and also more compact in terms of circuit depth than fixed-ansatze approaches. A variant of this approach—

labelled Overlap-ADAPT-VQE²⁰ – was recently introduced for quantum state preparation. The Overlap-ADAPT-VQE algorithm iteratively generates a compact approximation of a target wave function through a quasi-greedy procedure that maximises, at each iteration, the overlap of the current iterate with the target. This is achieved by adding on-the-fly, the most relevant unitary operator from a finite-size pool of admissible operators, with a selection criterion based on the gradient of the overlap of the ansatz with the target. Note that whether the Overlap-ADAPT-VQE ansatz evolves within the symmetry-relevant subspace of the target depends on the choice of the operator pool. Pools made of fermionic operators adhere to all the desired symmetries,¹⁹ which facilitates the convergence to the target state but comes at the expense of requiring more quantum gates per operator. Conversely, Qubit-Excitation-Based,^{21,22} Qubit,²³ or Minimal ZY²³ pools may respect only a subset of these symmetries or none at all, but they are more CNOT-efficient. The Overlap-ADAPT-VQE workflow and the associated details of the aforementioned operator pools are provided in the Appendix.

Despite a rather intuitive structure, variational quantum state preparation algorithms face scalability issues because they rely on heuristic classical optimization processes that are likely to become exponentially complex as the number of qubits grows.²⁴ Indeed, the optimization problem is non-convex and plagued by multiple local minima and barren plateaus,²⁵ which so far limited the applicability of variational QSP algorithms to rather simple quantum systems. Moreover, the computational complexity of finding optimal parameters in variational QSP algorithms cannot be easily characterised. Recently, significant research attention directed towards non-variational methods for quantum state preparation,^{26–29} particularly when the state to be prepared exhibits distinct structural traits or symmetries.^{8,28,30–34} As a result, sparse quantum state preparation algorithms offer an interesting alternative for the preparation of SCI wave functions, as they are deterministic and come with a significantly reduced classical computational complexity. We propose in Table 1a, a non-exhaustive list of

sparse quantum state preparation algorithms and associated complexities. Additionally, the circuit depth directly impacts the execution time, which must be shorter than the qubit decoherence time to obtain meaningful results. To the best of our knowledge and with respect to these last points, these methods are among the most efficient. By parallelizing the computation with ancilla qubits, the method from Xiao-Ming Zhang et al.³⁵ gets the lowest classical preprocessing overhead and circuit depth. Gleinig et al.³³ introduced an algorithm that requires no ancilla qubit at the expense of a classical preprocessing with a quadratic-scaling complexity. Fomichev et al.³⁶ introduced a method using Quantum Read-Only Memory which exhibits a CNOT-count that scales superlinearly with the sparsity including a logarithmic number of ancillas. Tubman et al.⁸ and De Veras et al.³⁴ have both introduced sparse QSP algorithms that employ a single ancilla qubit and possess linear complexity with respect to the sparsity of the target. The latter method, called CVO-QRAM, will be used in the following numerical simulations.

Table 1: Performance of common sparse state preparation methods.

Method	Classical preprocessing	CNOT count	Circuit Depth	Ancillas
CVO-QRAM ³⁴	$\mathcal{O}(M \log M + nM)$	$\sum_{t=1}^n \mu_t (8t - 4) - t_{\max}$	$\mathcal{O}(nM)$	1
Gleinig et al. ³³	$\mathcal{O}(M^2 \log(M)n)$	$\mathcal{O}(nM)$	$\mathcal{O}(nM)$	0
Tubman et al. ⁸		$\mathcal{O}(nM)$	$\mathcal{O}(nM)$	1
Zhang et al. ³⁵	$\mathcal{O}(nM)$	[very large]	$\Theta(\log(nM))$	$\mathcal{O}(nM \log M)$
Fomichev et al. ³⁶	$\mathcal{O}(M^3)$	$\mathcal{O}(M \log M)$	$\mathcal{O}(M \log M)$	$\mathcal{O}(\log M)$

(a) With respect to the target state, M denotes the sparsity, n the number of qubits involved, μ_t is the number of determinants with t bits of value 1 and t_{\max} is the highest value of t with $\mu_t \neq 0$.

The study presented in this Letter aims to compare the aforementioned state-of-the-art variational and non-variational approaches to sparse quantum state preparation on the criteria of circuit depth and classical pre-processing complexity. Our numerical experiments consist of preparing ground states of hydrogen chains, these molecular systems having an established reputation as prototypical strongly correlated systems with multi-determinantal character.³⁷ The linear hydrogen chains that we consider are stretched with an interatomic distance of 5.0 Å. The target ground states are obtained via CIPSI^{15,16} SCI simulations carried out on the Quantum Package³⁸ software, using a minimal STO-3G basis set, and

up to the challenging case of H_{14} , whose quantum encoding requires the significant count of 28 qubits. Figure 1a emphasizes, as anticipated, the exponential growth in the number of determinants needed to represent the ground-state of increasingly large hydrogen chains.

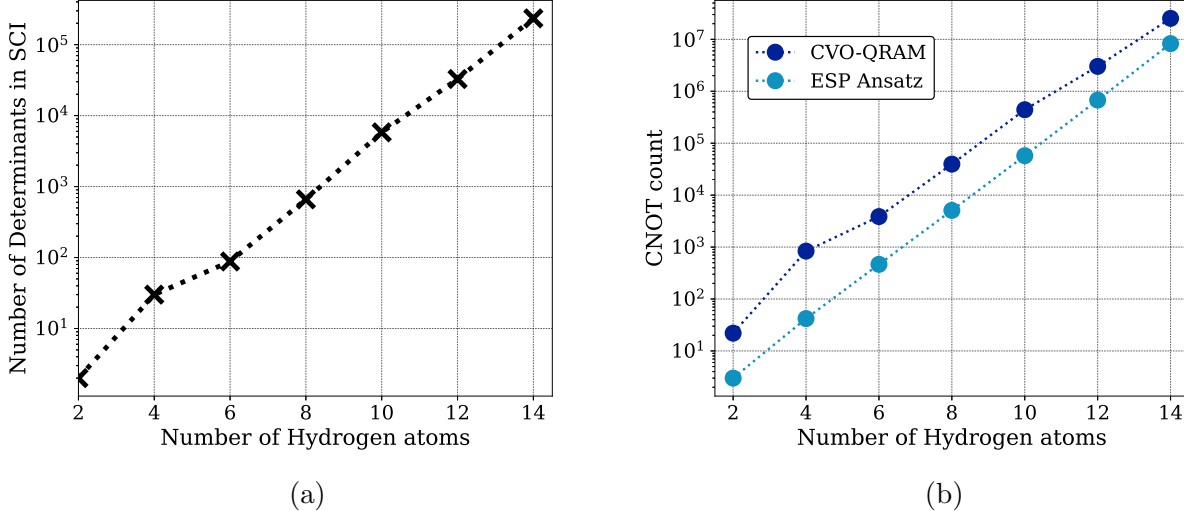


Figure 1: Determinants count (a) and CNOT count (b) in the SCI representation of linear H_n chains. The CNOT count has been established using CVO-QRAM loader and ESP Ansatz as state preparation method.

In Figure 1b, we display the number of CNOT gates required to construct a quantum circuit that encodes the Full-CI wave functions of hydrogen chains. These quantum circuits are obtained using the CVO-QRAM method and the Efficient Symmetry-Preserving (ESP) ansatz as quantum state preparation algorithms applied to the CIPSI ground state as a target. While the former approach substantially lowers the CNOT count compared to the CVO-QRAM method, it is crucial to emphasize that the ESP Ansatz is built upon certain underlying assumptions. First, the convergence of this optimization process cannot be guaranteed, giving rise to system-dependence, while CVO-QRAM ensures systematic success. Second, variational QSP via ESP Ansatz is likely to be of *at least* exponential complexity with the system size. In either scenario, performing QSP for such target states presents challenges, with impractical computational cost in one case and large CNOT overhead detrimental to the subsequent quantum post-treatment in the other.

The CVO-QRAM and ESP quantum state preparation results suggest that preparing compact approximations of the target state might be a natural option. Notably, variational methods can progressively approach the solution, allowing access to ansatz wave functions of arbitrary precision with arbitrary circuit depth and classical computational time. Adaptive variational algorithms have notably showcased their effectiveness compared to fixed-ansatz techniques in the realm of approximate ground state preparation. Specifically, the Overlap-ADAPT-VQE has previously been applied to QSP of SCI-wave functions,²⁰ making it a suitable choice for the forthcoming simulations. We carry out Overlap-ADAPT-VQE simulations with the linear H_{14} ground state as target on 28 qubits, and using two common operator pools, namely Qubit-Excitation-Based- and Qubit-pool, whose details are given in appendix. Such large computations are made possible thanks to the use of the in-house GPU-accelerated Hyperion quantum emulator. To ensure a fair comparison with CVO-QRAM, which performs exact state preparation, we prepare a range of approximated states of the linear H_{14} ground state. The approximation involves cropping the smallest coefficients of the target and renormalising, guaranteeing minimal sparsity for an arbitrary high overlap. We display in Figure 2a the absolute weight of each Slater determinant in the expansion of the ground state of the H_{14} linear hydrogen chain. Note that for the H_{14} system, relying on a single determinant initialisation yields at most a modest 4.10^{-2} overlap with the ground state. Moreover, Figure. 2b presents the associated absolute sum of CI squared coefficients, highlighting the need for a multi-determinant initial state.

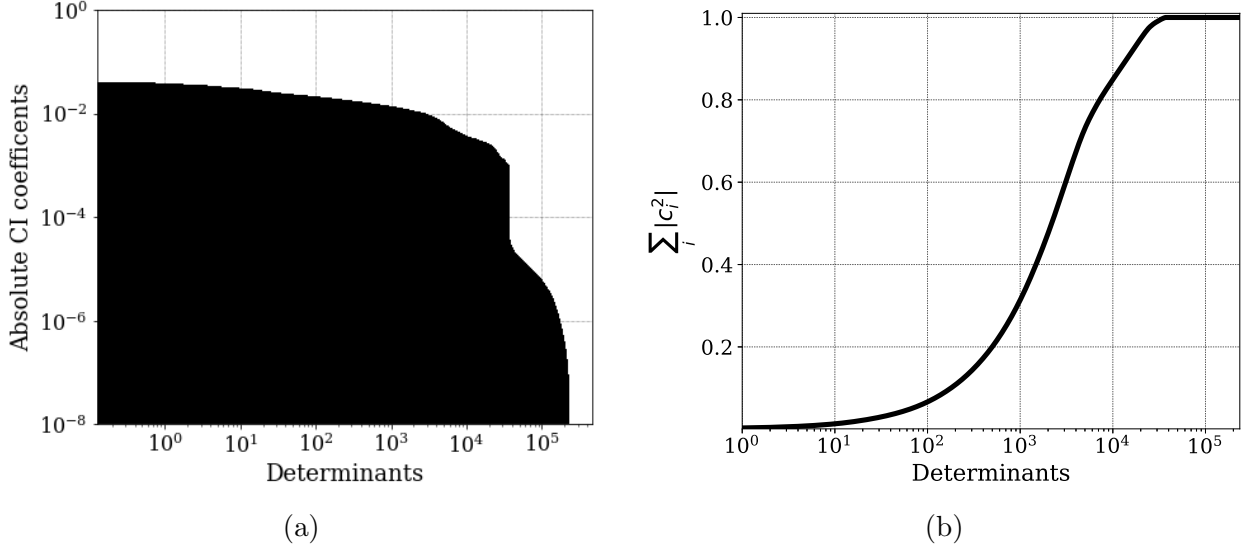


Figure 2: (a) Absolute CI coefficient of each Slater determinant in the Selected-CI expansion of linear H_{14} ground state wave function. (b) Associated absolute sum of CI squared coefficients.

The resulting CNOT count of QSP via CVO-QRAM and Overlap-ADAPT for various levels of approximations are given in Figure 3a. The adaptive variational approach leads to significantly reduced CNOT count for any level of fidelity. The CVO-QRAM approach is likely to dominate in preparing the exact target, as the variational approach may struggle in reaching full convergence with affordable classical computing cost. Indeed, Figure. 3b shows the convergence profile of the Overlap-ADAPT simulations and suggests the presence of a potentially significant plateau for reaching a perfect overlap with the target. Nevertheless, the majority of studies typically regard an overlap exceeding 0.5 with the ground state as sufficiently high for a Quantum Phase Estimation (QPE) initial state. This perspective makes the exact state preparation approach via CVO-QRAM unsuitable for these applications. In contrast, Overlap-ADAPT-VQE smoothly grows ansätze of over 95% fidelity with a system characterised by strong correlation. The associated circuit involves no more than a few thousand CNOT gates, a highly reasonable resource in the context of the early-fault tolerant era. We anticipate being able to replicate these outcomes in both resource utilisation and accuracy for even larger molecules, particularly those of interest that are beyond

classical simulation capabilities.

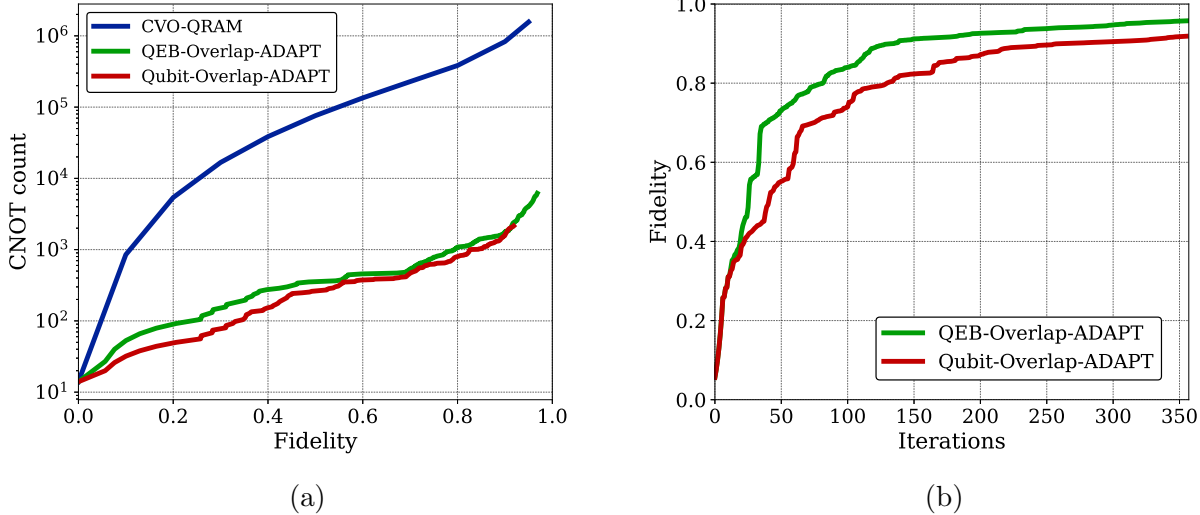


Figure 3: (a) CNOT-count for approximate QSP of ground state wave function of linear H_{14} displayed in 2, using CVO-QRAM and Overlap-ADAPT-VQE as QSP methods. (b) Fidelity of the Overlap-ADAPT-VQE ansatz over the iterations for the same target.

By generating a compact quantum circuit that encodes the best classically-derived wave function, we secure an initial quantum state with strong overlap with the sought-after ground state of the system. This initial state preparation will greatly facilitate a following quantum post-treatment, such as QPE, which offers asymptotic advantage in determining the ground state energy compared to classical approaches.

The key takeaway is that, even for chemical systems of prime hardness,³⁹ quantum state preparation of accurate initial state is a straightforward task using Overlap-ADAPT-VQE, which produces quantum circuits with insignificant circuit depth compared to the subsequent QPE process. We remark that in a broader context, sparse QSP methods are used for a range of applications, including Hamiltonian simulation with either linear combination of unitary operators⁴⁰ or qubitization,⁴¹ data loading for quantum machine learning⁴² or even solving linear system of equations.⁴³ Overlap-ADAPT-VQE may therefore offer a practical approach for any such algorithm involving classical data loading by allowing the use of an operator pool tailored to the target state's characteristics.

Technical Appendix

The Hyperion High-Performance State-Vector Emulator

Hyperion⁴⁴ is a quantum computing state-vector emulator package dedicated to quantum chemistry. It uses classical hardware and is massively parallel thanks to an efficient multi-GPU (GPU=Graphics Processing Unit) implementation. High performance is ensured by an ensemble of fast custom CUDA sparse linear algebra libraries, which act on the native quantum chemistry algorithms to accelerate Hyperion’s exact/noiseless simulations. For example, using a single DGX-A100 node (8 X A100 GPUs, 40Gb of memory/GPU), we have been able to carry out a 28 qubits Overlap-ADAPT-VQE simulation producing over 350 iterations within 5 days. The fidelity of the ansatz with respect to the H_{14} target state is plotted with respect to the iterates in Figure. 3b. Further details about Hyperion will be given in a forthcoming publication.

Double Sparse Quantum State Preparation

Even though it is unclear how to prepare an arbitrary state of 2^n complex amplitudes with a cost which is not exponential with the number of qubits n , the problem of loading a number M of complex amplitudes was proven to have satisfying solutions scaling linearly with M such as the CVO-QRAM method.³⁴ This algorithm consists in loading sequentially the classical data by performing controlled rotations using one ancilla qubit. The algorithm is presented and the correctness is proven recursively as follows.

Define the amplitude remaining to be loaded by $\gamma_0 = 1$, $\gamma_{k+1} = \gamma_k - |x_{k+1}|^2$ for $0 \leq k \leq M - 1$. Notice that by normalization of the input data, $\gamma_{M-1} = 0$. Then, for each k , define the unitary:

$$U^{(x_k, \gamma_k)} = \frac{1}{\sqrt{\gamma_k}} \begin{pmatrix} \sqrt{\gamma_k - |x_k|^2} & x_k \\ x_k^* & \sqrt{\gamma_k - |x_k|^2} \end{pmatrix}.$$

Algorithm 1: CVO-QRAM - Complex Data Storage Algorithm

```

input : data =  $\{x_k, p_k\}_{k=0}^{M-1}$ 
output:  $|m\rangle = \sum_{k=0}^{M-1} x_k |p_k\rangle$ 

1 cvoqram (data,  $|\psi\rangle$ ):
2    $|\psi_{0_0}\rangle = |u\rangle |m\rangle = |1; 0, \dots, 0\rangle$ 
3   foreach  $(x_k, p_k) \in \text{data}$  do
4      $t = \text{The number of bits with value 1 in the pattern } p_k$ 
5      $l = \text{a list containing the positions of } p_k \text{ where } p_k[j] = 1.$ 
6      $|\psi_{k_1}\rangle = \prod_{l_i \in l} CX_{(u, m[l_i])} |\psi_{k_0}\rangle$ 
7      $|\psi_{k_2}\rangle = C^t U^{(x_k, \gamma_k)}_{(m[l_0, l_1, \dots, l_{t-1}], u)} |\psi_{k_1}\rangle$ 
8     if  $k \neq M-1$  then
9        $|\psi_{k_3}\rangle = \prod_{l_i \in l} CX_{(u, m[l_i])} |\psi_{k_2}\rangle$ 
10  return  $|m\rangle$ 

```

The algorithm correctness is proven using the following loop invariant H_k , $k = 0 \dots M-1$:

H_k : Right before loading (x_k, p_k) , line 3, the state of the system is $|\psi_{k_0}\rangle = \sum_{j=0}^{k-1} x_j |0, p_j\rangle + \sqrt{\gamma_k} |1, 0\rangle$.

For $k = 0$, H_0 holds vacuously. Let us check for $k < M-1$, the for loop maintains the property. Assume that H_k is verified. Then, simply compute:

$$\begin{aligned}
|\psi_{k_1}\rangle &= \sum_{j=0}^{k-1} x_j |0, p_j\rangle + \sqrt{\gamma_k} |1, p_k\rangle \\
|\psi_{k_2}\rangle &= \sum_{j=0}^{k-1} x_j |0, p_j\rangle + \sqrt{\gamma_k} \left(\frac{x_k}{\sqrt{\gamma_k}} |0, p_k\rangle + \frac{\sqrt{\gamma_{k+1}}}{\sqrt{\gamma_k}} |1, p_k\rangle \right) \\
&= \sum_{j=0}^k x_j |0, p_j\rangle + \sqrt{\gamma_{k+1}} |1, p_k\rangle \\
|\psi_{k_3}\rangle &= \sum_{j=0}^k x_j |0, p_j\rangle + \sqrt{\gamma_{k+1}} |1, 0\rangle
\end{aligned} \tag{4}$$

Thus, the property is maintained. In order to show that the procedure ends well, simply

notice $|\gamma_{M-1}\rangle = 0$ since the input data must be normalized (without loss of generality).

The CVO-QRAM method needs two steps of classical pre-processing. First, given an input with M patterns to load, the classical device must first sort the input patterns with cost $\mathcal{O}(M \log M)$. Then, it creates the circuits associated to the $U^{(x_k, \gamma_k)}$ with total cost $\mathcal{O}(nM)$. The total, classical cost is $\mathcal{O}(M \log M + nM)$. In terms of quantum gates, the number of CNOT gates to prepare a state is

$$\sum_{t=1}^n \mu_t (8t - 4) - t_{\max},$$

where μ_t is the number of input patterns p_k with t bits with value 1 in the binary string and t_{\max} is the highest value of t with $\mu_t \neq 0$.

Overlap-ADAPT-VQE

The general workflow of the Overlap ADAPT-VQE^{20,45} algorithm is as follows:

Algorithm 2: Overlap-ADAPT-VQE - Variational Quantum State Preparation

input : initial state $|\psi_0\rangle$, target state $|\phi_T\rangle$, pool of operators \mathcal{A} , convergence threshold ϵ
output: ansatz $|\psi(\theta)\rangle$ such as $|\langle\psi(\theta)|\phi_T\rangle| < \epsilon$

1 Overlap-ADAPT-VQE($|\psi_0\rangle$, $|\phi_T\rangle$, \mathcal{A} , ϵ):
2 $n \leftarrow 1$
3 **while** $S_n = |\langle\psi_n(\theta)|\Psi_T\rangle| > \epsilon$ **do**
4 **foreach** $A_k \in \mathcal{A}$ **do**
5 Measure gradients $g_{A_k} \leftarrow \left| \frac{\partial S_{n,A_k}(\theta)}{\partial \theta} \right| \Big|_{\theta=0}$
6 $i \leftarrow$ index of the largest element of \tilde{g}
7 Pick best operator $A_n \leftarrow A_i$
8 Grow Ansatz $|\psi_n\rangle \leftarrow A_n |\psi_{n-1}\rangle$
9 Optimise Ansatz $\theta^{\text{opt}} = \underset{\theta=(\theta_1, \dots, \theta_n)}{\text{argmin}} |\langle\psi_n(\theta)|\Psi_T\rangle|$
10 $\theta \leftarrow \theta^{\text{opt}}$
11 Iterate $n \leftarrow n + 1$
12 **return** $|\psi_n(\theta)\rangle$

Operator Pools

The literature contains a wide range of operator pools for ADAPT-like algorithms and VQEs. Some are chemically-inspired and ensure that the ansatz preserves the symmetry of the target state, while others prioritize hardware efficiency and minimize the number of operators used.^{23,46} This section intends to offer a concise introduction to the two operator pools that have been used in prior numerical simulations.

The Qubit Excitation-based Pool

The Qubit excitation-based (QEB) pool is widely used for simulating quantum chemical systems²¹ because it preserves spin and number of particles while still being fairly hardware efficient. The QEB pool consists of so-called single-qubit and double-qubit excitation operators which take the form

$$A_{pq} = \frac{1}{2} (X_q Y_p - Y_p X_q). \quad (5)$$

and

$$A_{pqrs} = \frac{1}{8} (X_r Y_s X_p X_q + Y_r X_s X_p X_q + Y_r Y_s Y_p X_q + Y_r Y_s X_p Y_q - X_r X_s Y_p X_q - X_r X_s X_p Y_q - Y_r X_s Y_p Y_q - X_r Y_s Y_p Y_q). \quad (6)$$

The variables p, q, r, s represent qubit indices, and X_p and Y_p represent the standard one-qubit Pauli gates applied to qubit p . Therefore, the single-qubit generator A_{pq} operates between individual qubits p and q , while the double-qubit generator A_{pqrs} operates between the qubit pairs (p, q) and (r, s) . The computation of parametric exponentiation for QEB operators is straightforward, and the resulting unitary operators come with well established CNOT-optimized circuit implementations detailed in Figure. ??.

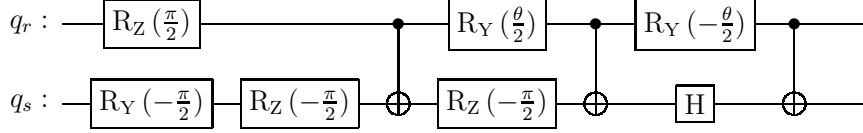


Figure 4: A quantum circuit performing a generic single-qubit evolution.⁴⁷

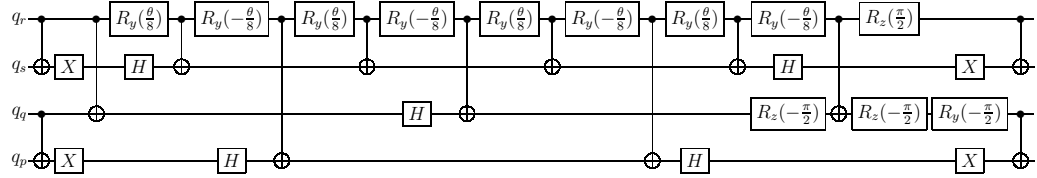


Figure 5: A quantum circuit performing a generic double-qubit evolution.⁴⁷

The Qubit Hardware-efficient Pool

The Qubit hardware-efficient²² pool instead uses decomposed single and double excitation operators which are of the form

$$B_{pq} = X_q Y_p \quad (7)$$

and

$$\begin{aligned} B_{pqrs}^{(1)} &= X_r Y_s X_p X_q, & B_{pqrs}^{(2)} &= Y_r X_s X_p X_q, & B_{pqrs}^{(3)} &= Y_r Y_s Y_p X_q, & B_{pqrs}^{(4)} &= Y_r Y_s X_p Y_q, \\ B_{pqrs}^{(5)} &= X_r X_s Y_p X_q, & B_{pqrs}^{(6)} &= X_r X_s X_p Y_q, & B_{pqrs}^{(7)} &= Y_r X_s Y_p Y_q, & B_{pqrs}^{(8)} &= X_r Y_s Y_p Y_q, \end{aligned} \quad (8)$$

where p, q, r, s again denote qubit indices and X_p and Y_p are one-qubit Pauli gates acting on qubit p . Note that the qubit hardware-efficient pool does not preserve particle and spin conservation of the ansatz, which may result in convergence difficulties due to the violation of such crucial system symmetries. However, prior numerical simulations employing the qubit hardware-efficient pool have produced ansatze that require fewer CNOT operations for implementation on quantum hardware when compared to ansatz wave functions based on the QEB pool.

Acknowledgement

We thank Muhammad Hassan and Yvon Maday (LJLL, Sorbonne Université) for providing feedback on the composition of this paper. The DGX-A100 GPUs computations have been performed thanks to the support of the European Research Council (ERC) under the European Union’s Horizon 2020 research and innovation program (grant agreement No 810367), project EMC2 (JPP). Support from the PEPR EPiQ and HQI programs is also acknowledged (JPP).

References

- (1) Helgaker, T.; Jorgensen, P.; Olsen, J. *Molecular electronic-structure theory*; John Wiley & Sons, 2013.
- (2) Peruzzo, A.; McClean, J.; Shadbolt, P.; Yung, M.-H.; Zhou, X.-Q.; Love, P. J.; Aspuru-Guzik, A.; O'brien, J. L. A variational eigenvalue solver on a photonic quantum processor. *Nature Communications* **2014**, *5*, 1–7.
- (3) Kitaev, A. Y. Quantum measurements and the Abelian stabilizer problem. *arXiv preprint quant-ph/9511026* **1995**,
- (4) Nielsen, M. A.; Chuang, I. L. *Quantum computation and quantum information*; Cambridge University Press, 2010.
- (5) Aspuru-Guzik, A.; Dutoi, A. D.; Love, P. J.; Head-Gordon, M. Simulated quantum computation of molecular energies. *Science* **2005**, *309*, 1704–1707.
- (6) Whitfield, J. D.; Biamonte, J.; Aspuru-Guzik, A. Simulation of electronic structure Hamiltonians using quantum computers. *Molecular Physics* **2011**, *109*, 735–750.
- (7) Tilly, J.; Chen, H.; Cao, S.; Picozzi, D.; Setia, K.; Li, Y.; Grant, E.; Wossnig, L.;

Rungger, I.; Booth, G. H.; others The variational quantum eigensolver: a review of methods and best practices. *Physics Reports* **2022**, *986*, 1–128.

(8) Tubman, N. M.; Mejuto-Zaera, C.; Epstein, J. M.; Hait, D.; Levine, D. S.; Huggins, W.; Jiang, Z.; McClean, J. R.; Babbush, R.; Head-Gordon, M.; Whaley, K. B. Postponing the orthogonality catastrophe: efficient state preparation for electronic structure simulations on quantum devices. *arXiv preprint arXiv:1809.05523* **2018**,

(9) Dalzell, A. M.; McArdle, S.; Berta, M.; Bienias, P.; Chen, C.-F.; Gilyén, A.; Hann, C. T.; Kastoryano, M. J.; Khabiboulline, E. T.; Kubica, A.; others Quantum algorithms: A survey of applications and end-to-end complexities. *arXiv preprint arXiv:2310.03011* **2023**,

(10) Lee, S.; Lee, J.; Zhai, H.; Tong, Y.; Dalzell, A. M.; Kumar, A.; Helms, P.; Gray, J.; Cui, Z.-H.; Liu, W.; others Evaluating the evidence for exponential quantum advantage in ground-state quantum chemistry. *Nature Communications* **2023**, *14*, 1952.

(11) Plesch, M.; Brukner, Č. Quantum-state preparation with universal gate decompositions. *Physical Review A* **2011**, *83*, 032302.

(12) Grover, L.; Rudolph, T. Creating superpositions that correspond to efficiently integrable probability distributions. *arXiv preprint quant-ph/0208112* **2002**,

(13) Mottonen, M.; Vartiainen, J. J.; Bergholm, V.; Salomaa, M. M. Transformation of quantum states using uniformly controlled rotations. *arXiv preprint quant-ph/0407010* **2004**,

(14) Nesbet, R. K. Configuration Interaction in Orbital Theories. *Proc. R. Soc. A* **1955**, *230*, 312–321.

(15) Huron, B.; Malrieu, J. P.; Rancurel, P. Iterative perturbation calculations of ground and

excited state energies from multiconfigurational zeroth-order wavefunctions. *Journal of Chemical Physics* **1973**, *58*, 5745–5759.

(16) Evangelisti, S.; Daudey, J.-P.; Malrieu, J.-P. Convergence of an improved CIPSI algorithm. *Journal of Chemical Physics* **1983**, *75*, 91 – 102.

(17) Jordan, P.; Wigner, E. P. *The Collected Works of Eugene Paul Wigner*; Springer, 1993; pp 109–129.

(18) Gard, B. T.; Zhu, L.; Barron, G. S.; Mayhall, N. J.; Economou, S. E.; Barnes, E. Efficient symmetry-preserving state preparation circuits for the variational quantum eigensolver algorithm. *npj Quantum Information* **2020**, *6*, 10.

(19) Grimsley, H. R.; Economou, S. E.; Barnes, E.; Mayhall, N. J. Adapt-vqe: An exact variational algorithm for fermionic simulations on a quantum computer. *arXiv preprint arXiv:1812.11173* **2018**,

(20) Feniou, C.; Hassan, M.; Traoré, D.; Giner, E.; Maday, Y.; Piquemal, J.-P. Overlap-ADAPT-VQE: practical quantum chemistry on quantum computers via overlap-guided compact Ansätze. *Communications Physics* **2023**, *6*, 192.

(21) Yordanov, Y. S.; Armaos, V.; Barnes, C. H.; Arvidsson-Shukur, D. R. Qubit-excitation-based adaptive variational quantum eigensolver. *Communications Physics* **2021**, *4*, 1–11.

(22) Ryabinkin, I. G.; Yen, T.-C.; Genin, S. N.; Izmaylov, A. F. Qubit coupled cluster method: a systematic approach to quantum chemistry on a quantum computer. *Journal of chemical theory and computation* **2018**, *14*, 6317–6326.

(23) Tang, H. L.; Shkolnikov, V. O.; Barron, G. S.; Grimsley, H. R.; Mayhall, N. J.; Barnes, E.; Economou, S. E. Qubit-Adapt-Vqe: An adaptive algorithm for constructing hardware-efficient ansätze on a quantum processor. *PRX Quantum* **2021**, *2*, 020310.

(24) Astrakhantsev, N.; Mazzola, G.; Tavernelli, I.; Carleo, G. Phenomenological theory of variational quantum ground-state preparation. *Phys. Rev. Res.* **2023**, *5*, 033225.

(25) McClean, J. R.; Boixo, S.; Smelyanskiy, V. N.; Babbush, R.; Neven, H. Barren plateaus in quantum neural network training landscapes. *Nature communications* **2018**, *9*, 4812.

(26) Araujo, I. F.; Park, D. K.; Petruccione, F.; da Silva, A. J. A divide-and-conquer algorithm for quantum state preparation. *Scientific reports* **2021**, *11*, 6329.

(27) Araujo, I. F.; Blank, C.; Araújo, I. C.; da Silva, A. J. Low-rank quantum state preparation. *IEEE Transactions on Computer-Aided Design of Integrated Circuits and Systems* **2023**,

(28) Zhang, X.-M.; Li, T.; Yuan, X. Quantum State Preparation with Optimal Circuit Depth: Implementations and Applications. *Phys. Rev. Lett.* **2022**, *129*, 230504.

(29) Sun, X.; Tian, G.; Yang, S.; Yuan, P.; Zhang, S. Asymptotically optimal circuit depth for quantum state preparation and general unitary synthesis. *IEEE Transactions on Computer-Aided Design of Integrated Circuits and Systems* **2023**,

(30) Zylberman, J.; Debbasch, F. Efficient Quantum State Preparation with Walsh Series. *arXiv preprint arXiv:2307.08384* **2023**,

(31) Holmes, A.; Matsuura, A. Y. Efficient quantum circuits for accurate state preparation of smooth, differentiable functions. 2020 IEEE International Conference on Quantum Computing and Engineering (QCE). 2020; pp 169–179.

(32) Marin-Sanchez, G.; Gonzalez-Conde, J.; Sanz, M. Quantum algorithms for approximate function loading. *Physical Review Research* **2023**, *5*, 033114.

(33) Gleinig, N.; Hoefler, T. An Efficient Algorithm for Sparse Quantum State Preparation. 2021 58th ACM/IEEE Design Automation Conference (DAC). 2021; pp 433–438.

(34) de Veras, T. M. L.; da Silva, L. D.; da Silva, A. J. Double sparse quantum state preparation. *Quantum Information Processing* **2022**, *21*, 204.

(35) Zhang, X.-M.; Li, T.; Yuan, X. Quantum State Preparation with Optimal Circuit Depth: Implementations and Applications. *Physical Review Letters* **2022**, *129*.

(36) Fomichev, S.; Hejazi, K.; Zini, M. S.; Kiser, M.; Morales, J. F.; Casares, P. A. M.; Delgado, A.; Huh, J.; Voigt, A.-C.; Mueller, J. E.; Arrazola, J. M. Initial state preparation for quantum chemistry on quantum computers. *arXiv preprint arXiv:2310.18410* **2023**,

(37) Stair, N. H.; Evangelista, F. A. Exploring Hilbert space on a budget: Novel benchmark set and performance metric for testing electronic structure methods in the regime of strong correlation. *The Journal of Chemical Physics* **2020**, *153*, 104108.

(38) Garniron, Y. et al. Quantum Package 2.0: An Open-Source Determinant-Driven Suite of Programs. *Journal of Chemical Theory and Computation* **2019**, *15*, 3591–3609, PMID: 31082265.

(39) Choi, S.; Yen, T.-C.; Izmaylov, A. F. Improving Quantum Measurements by Introducing “Ghost” Pauli Products. *Journal of Chemical Theory and Computation* **2022**, *18*, 7394–7402.

(40) Childs, A. M.; Wiebe, N. Hamiltonian simulation using linear combinations of unitary operations. *arXiv preprint arXiv:1202.5822* **2012**,

(41) Low, G. H.; Chuang, I. L. Hamiltonian simulation by qubitization. *Quantum* **2019**, *3*, 163.

(42) Zhao, Z.; Fitzsimons, J. K.; Rebentrost, P.; Dunjko, V.; Fitzsimons, J. F. Smooth input preparation for quantum and quantum-inspired machine learning. *Quantum Machine Intelligence* **2021**, *3*, 14.

(43) Harrow, A. W.; Hassidim, A.; Lloyd, S. Quantum algorithm for linear systems of equations. *Physical Review Letters* **2009**, *103*, 150502.

(44) Adjoua, O.; Feniou, C.; et al. Sorbonne Université and CNRS and Qubit Pharmaceuticals. 2023.

(45) Feniou, C.; Claudon, B.; Hassan, M.; Courtat, A.; Adjoua, O.; Maday, Y.; Piquemal, J.-P. Greedy Gradient-free Adaptive Variational Quantum Algorithms on a Noisy Intermediate Scale Quantum Computer. *arXiv preprint arXiv:2306.17159* **2023**,

(46) Kandala, A.; Mezzacapo, A.; Temme, K.; Takita, M.; Brink, M.; Chow, J. M.; Gambetta, J. M. Hardware-efficient variational quantum eigensolver for small molecules and quantum magnets. *Nature* **2017**, *549*, 242–246.

(47) Yordanov, Y. S.; Arvidsson-Shukur, D. R.; Barnes, C. H. Efficient quantum circuits for quantum computational chemistry. *Physical Review A* **2020**, *102*, 062612.